Are Atrial Fibrillation Dominant Frequency Areas the Source of Dominant Excitation Patterns? A Left Atrial Panoramic View

Frederique J Vanheusden[1], Ahmed Ulusow[1], Gavin S Chu[2], Xin Li[2], João L Salinet[3], Peter J Stafford[2], G André Ng[2,4], Fernando S Schlindwein[2,4]

[1]Nottingham Trent University, Nottingham, United Kingdom
[2]University of Leicester, Leicester, United Kingdom
[3]Federal University of ABC, São Paulo, Brazil
[4]National Institute for Health Research Leicester Cardiovascular Biomedical Research Centre, Leicester, UK

Abstract

Atrial fibrillation (AF) catheter ablation success depends on the possibility to accurately determine areas on the atrial endocardium at which AF activation originates. One way to determine if major AF activation pathways originate at identified source is through causality analysis. This work assessed to what extent left atrial highest dominant frequency (HDF) areas can be identified as sources of activation pathways in 10 male subjects suffering from persistent AF. Virtual electrograms were collected from 64 endocardial locations for at least 5 minutes. Frequency and causality were analyzed on 4 s signal segments Causality was assessed using the directed transfer function (DTF) algorithm, and AF activation sources were identified as endocardial locations of which the VEGM signal had high influence on other VEGM signals. Co-localization of high influence and HDF areas was evaluated for different area overlap and spectral organisation (OI) thresholds. Results show that, on average, good overlap only existed in 64.6% (± 8.8%) over all subject using the lowest threshold settings. Good overlap rates reduced with more conservative thresholds. This indicates that HDF areas might not always identify origins of main AF activation pathways.

1. Introduction

Finding the appropriate atrial area to target in catheter ablation of persistent atrial fibrillation (AF) remains challenging. Many algorithms have been suggested in recent years [1-3], yet the rate of ablation success remains unsatisfactory low. Reasons for this are an incomplete understanding of the underlying pathophysiology of AF [4], as well as variations in algorithm implementations between different (commercialized) software [5]. One particular hypothesis suggests that areas of high dominant frequency (HDF) are suitable ablation targets [2]. An early study showed that, using a contact-mapping catheter, ablation of local HDF areas predicted long-term maintenance of sinus rhythm [2].

HDF areas on their own do not provide information about the propagation of AF patterns, however. Knowledge of AF propagation over time would enhance understanding of the complex behavior of AF, and provide additional scrutiny about the relevance of HDF areas as AF sources. Granger causality analysis between atrial signals has previously shown causality analysis might improve specificity of source detection compared to HDF analysis [6]. In this study, data were collected using contact mapping, which only provides information about local HDF behavior. Some studies investigating HDF behavior using non-contact mapping have however suggested that HDF areas are not stable in time, moving across the atrial surface over time and often occurring simultaneously at various locations on the atrial endocardium [7]. It is therefore unclear if this pattern is valid taking into account this more complex panoramic HDF behavior.

The aim of this study was therefore to determine if a strong relationship between HDF areas and AF propagation patterns could also be observed when taking into account HDF behavior over the complete endocardial surface. For this purpose, the overlap of propagation sources as identified using the directed transfer function (DTF) algorithm [8] and HDF areas.

2. Methods

AF data were collected as described in previous work by our research group [9-10]. Briefly, left atrial virtual electrogram (VEGM) signals were collected from 10 male subjects (age range 36-76) referred for first-time ablation of persistent AF. For all subjects, 3D electro-anatomical mapping was performed. A 64-channel non-contact balloon catheter (EnSite, St Jude Medical, USA) collected

data for at least 5 minutes per subject at a sampling rate of 2034.5 Hz. From these data, VEGMs at 64 locations (nodes) on the left atrial endocardium were derived using built-in software. Data were exported after applying the software's default band-pass filter between 1 and 100 Hz. All subjects were in AF at the start of the procedure and under general anesthesia during the procedure. Ablation was performed by targeting HDF areas followed by standard pulmonary vein isolation (PVI). The local ethics committee approved the study and all procedures were performed with informed consent from the subjects.

2. Highest dominant frequency analysis

Data were processed offline in MATLAB R2018b (The MathWorks, USA). All data were resampled to 512 Hz. Ventricular activity was subtracted using the algorithm described by Salinet *et al.* [11]. Power spectra were created using a Fast Fourier Transform (FFT) of 4 s VEGM segments with an overlap of 50% between successive segments after applying a Hamming window. For each of the 64 VEGM signals in every 4 s segment, the dominant frequency (DF) was defined as the frequency with the maximum power in the interval between 4 and 10 Hz. For each segment, the area of HDF was defined as the area of VEGM signals including DF values within a +/-0.25 Hz range of the HDF value.

2.2 Causality analysis

Causality between VEGM signals was analyzed using a DTF algorithm [8]. The DTF algorithm allows to determine connectivity between VEGM signals in the frequency domain, visualizing both direct and indirect coupling between signals [12]. As described by Baccala *et al.* [12], the DTF algorithm first fits a multivariate autoregressive (AR) model of order p to the VEGM signals:

$$VEGM(n) = \sum_{l=1}^{p} A(l)VEGM(n-l) + \varepsilon(n) \qquad (1)$$

with $\varepsilon(n)$ being a noise term at the n^{th} sample. The coefficients composing $A(l)$, $a_{mk}(l)$ describe the effects of the m^{th} on the k^{th} VEGM signal after applying a lag of l samples. $A(l)$ can be converted to the frequency domain via:

$$\bar{A}_{mk}(\lambda) = \begin{cases} 1 - \sum_{l=1}^{p} a_{mk}(l)e^{-i2\pi\lambda l}, if\ m = k \\ -\sum_{l=1}^{p} a_{mk}(l)e^{-i2\pi\lambda l}, otherwise \end{cases} \qquad (2)$$

A transformation matrix $H_{mk}(\lambda) = \bar{A}_{mk}(\lambda)^{-1}(\lambda)$ can then be generated to calculate the DTF:

$$\gamma_{mk}(\lambda) = \frac{H_{mk}(\lambda)}{\sqrt{h'_m(\lambda)Ih_m(\lambda)}} \qquad (3)$$

with h_m the m$^{\text{th}}$ row of matrix H_{mk} and I an identity matrix.

For each 4 s segment, causality between VEGM signals was calculated for each frequency within the 4-10 Hz range. Influence ratios (IRs) between the m^{th} and k^{th} signal were determined based on previous work [6]:

$$IR = \frac{\gamma_{mk}}{\gamma_{mm}} \qquad (4)$$

The likelihood of a specific signal identifying a source of atrial activity was then determined by taking the average normalized IRs of this particular signal with all other signals. IRs were calculated for the HDF specific for each window. To determine if HDF areas indicated the same nodes as those with a high IR (HIR), the overlap between the HDF area and HIR area, including nodes directly neighboring these areas was determined. For each window, good overlap between both HDF and HIR areas was considered if the number of nodes covered by both areas was above a set 'overlapping threshold' (OT), indicating the number of overlapping nodes of HDF and HIR areas. OT was varied between 10 and 50%.

2.3 Effect of DF stability

A factor that can heavily affect DF behavior and therefore the location of the HDF area is the strength of the DF peak in the power spectrum (DF stability [7, 9-10]). One way of assessing this DF stability is through applying an organization index threshold (OI [9]). The effect of applying an OI threshold on overlap between HDF area and IR areas was therefore determined by varying the OI between 0.2 and 0.5.

2.4 Statistics

The percentage of windows with good overlap were evaluated for each OT and OI setting. Analysis of variance (ANOVA) was used to determine if the effect of changing OI and/or OT on the percentage of good overlap between HDF and HIR areas was significant at an alpha level of 0.05. This was followed with a post-hoc (Tukey) test for comparison between individual OI and OT values.

3. Results

HDF and causality analysis was performed on 148±8 4

s segments per subject. Overlap between HDF and HIR areas focused on causality at the HDF frequency were evaluated for each 4 s segment. Figure 1 shows an example of a segment for which a good overlap between areas was obtained (OI=0.2, OT=10%).

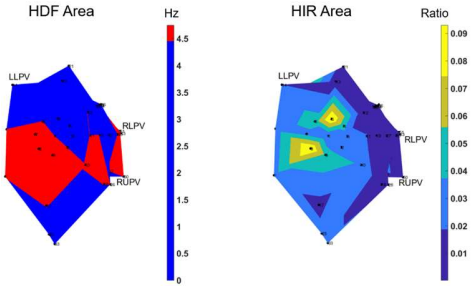

Figure 1: Example of a segment with a good HDF-HIR area overlap (OI threshold = 0.2, OT = 10%). LLPV: Left Lower Pulmonary Vein; RLPV: Right Lower Pulmonary Vein, RUPV: Right Upper Pulmonary Vein.

Figure 2 shows the same segment with different thresholds (OI=0.5, OT=50%). Here, no overlap is found between HDF and HIR areas.

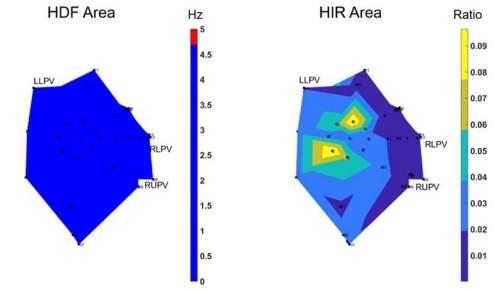

Figure 2: HDF and HIR area maps for the same window as in Figure 1, but with different threshold (OI = 0.5, OT = 50%). No overlap between HDF and HIR area is observed.

Figure 3 shows the average rate of 4 s segments for which a good overlap existed between the HDF and HIR areas over all subjects for different OI thresholds and OTs. Rates of 4 s segments with good overlap between HDF and HIR areas were highest for an OI threshold of 0.1 and OT of 10% (64.6% ± 8.8%, mean ± standard deviation). Furthermore, good overlap rate decreases with increased OI and overlap threshold.

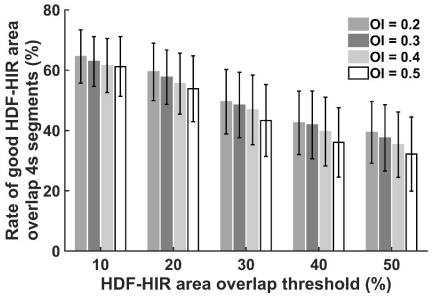

Figure 3: Average rate of windows with good overlap between HDF and HIR area for different OI and overlap thresholds. Error bars indicate standard deviation.

ANOVA showed that both OI ($p=0.041$) and OT ($p<0.005$) had a significant effect on the good overlap rate. The post-hoc test showed a significant effect if the OI threshold was changed from 0.2 to 0.5 only. For OT, significant differences in good overlap rate were observed when changing the OT from 10% to 40% or 50%, or when changing from 20% to 40% or 50%.

To determine if comparing HIR areas based on causality at the HDF value only induced bias, the procedure was repeated taking the average IRs over the entire DF frequency range (4-10 Hz). Figure 4 shows the results of good overlap rates for an OI threshold set at 0.4 and varying OT. No significant difference could be observed between overlap rates when HIR areas are calculated over the entire AF range against only the HDF value for each window (ANOVA, $p>0.05$). Similar results were achieved over the entire OI threshold range investigated.

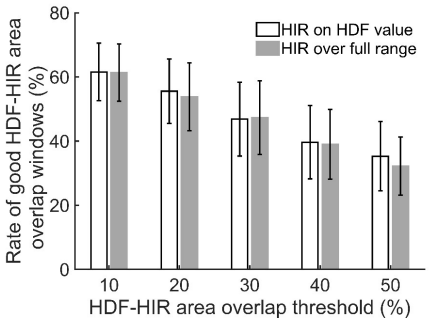

Figure 4: Comparison of overlap between HDF and HIR areas for causality analyzed on the HDF value only against the full AF frequency range. No significant difference was observed.

4. Discussion

As ablation of current target sources does not always lead to success, better understanding of what mechanism of the AF activation pathway these sources represent is required. Causality analysis allows to determine atrial locations at which atrial activity has strong influence over activity at other location on the atrial surface. Moreover, it allows to determine a directionality of activation patterns between areas, potentially providing insights about major activation pathways throughout the atria that cause AF [6].

Previous work has compared AF source identification based on Granger causality with sources identified by DF analysis in cases where a DF gradient could be observed [6]. This paper showed a good consistency between HDF areas and activation sources identified by causality based on contact mapping data. This study further investigated this coincidence between HDF and causality sources using data obtained simultaneously over the entire left atrium by

non-contact mapping, as previous studies have suggested HDF area instability which might make a conclusion about local DF behavior invalid [7]. Overlap between HDF and causality sources, measured using the DTF algorithm, was determined over 4 s segments. Results show that, at best, a fair overlap between HDF and causality sources could be obtained, using very tolerant area overlap and spectral organization thresholds. With more strict thresholds, the rate of windows for which a good overlap was achieved was lower than 50%. These results therefore do not fully agree with results from previous work [6], indicating that causality analysis might identify different targets for ablation than HDF.

One reason for this discrepancy could indeed be a higher complexity of the AF activation mechanism that cannot be fully appreciated through contact mapping of small atrial areas. Another reason for the difference could however be the lack of a left-to-right atrial DF gradient in our study cohort, which appears a necessary condition for successful ablation based on HDF targets [1]. Furthermore, although DTF might be considered a frequency domain-based form of Granger causality [8], causality analysis in this study was focused on the HDF only. Although no significant effect was seen when extending causality over the entire AF frequency range (4-10 Hz), analysis of causality on this filtered signal might differ from results obtained on an (unfiltered) time-domain signal [6]. Finally, both Granger causality and DTF algorithms do not distinguish between direct and indirect causal relations. Identified DTF sources might therefore indicate local pathways which are dependent on sources at other atrial areas. Future work should therefore focus on measuring only direct causal relationships, e.g. by using direct DTF algorithms [12].

5. Conclusion

This study investigated if HDF areas identify sources of AF activation pathways by determining how well these areas co-localize with areas of high influence on other atrial signals as assessed by a DTF algorithms. Results show that HDF areas do not always overlap with high influence areas, indicating that HDF areas might not always identify sources of main atrial activation pathways. However, the overlapping HDF and HIR regions found by the proposed method might indicate potential precise targets with fast activation that are truly driving slower regions as 'source', which could be important marks for AF initiation and maintenance.

Acknowledgments

This work falls under the portfolio of research conducted within the NIHR Leicester Biomedical Research Centre. XL received funding from the British Heart Foundation (PG/18/33/33780).

References

[1] K. Nademanee *et al.*, "A new approach for catheter ablation of atrial fibrillation: mapping of the electrophysiologic substrate," *J. Am. Coll Cardiol.*, vol. 43, no. 11, pp. 2044-2053, Jun 2004.

[2] F. Atienza *et al.*, "Real-time dominant frequency mapping and ablation of dominant frequency sites in atrial fibrillation with left-to-right frequency gradients predicts long-term maintenance of sinus rhythm," *Heart Rhythm*, vol. 6, no. 1, pp. 33-40, Jan 2009.

[3] S.M. Narayan *et al.*, "Clinical mapping approach to diagnose electrical rotors and focal impulse sources for human atrial fibrillation," *J. Cardiovasc. Electrophysiol.,* vol. 23, no. 5, pp. 447-454, May 2013.

[4] H. Oral *et al.*, "Pulmonary vein isolation for paroxysmal and persistent atrial fibrillation," *Circulation*, vol. 105, no. 9, pp. 1077-1081 Feb 2002.

[5] T.P. Almeida *et al.*, "Minimizing discordances in automated classification of fractionated electrograms in human persistent atrial fibrillation," *Med. Biol. Eng. Comput.*, vol. 54, no. 11, pp. 1695-1706, Nov 2016.

[6] M. Rodrigo *et al.*, "Identification of dominant excitation patterns and sources of atrial fibrillation by causality analysis," *Ann. Biomed. Eng.*, vol. 44, no. 8, pp. 2364-2376, Aug 2016.

[7] J.L. Salinet *et al.*, "Distinctive patterns of dominant frequency trajectory behavior in drug-refractory persistent atrial fibrillation: preliminary characterization of spatiotemporal instability," *J. Cardiovasc. Electrophysiol.*, vol. 25, no.4, pp. 371-379, Apr 2014.

[8] K.J. Blinowska, "Review of the methods of determination of directed connectivity from multichannel data," *Med. Biol. Eng. Comput.*, vol. 49, no. 5, pp. 521-529, Feb 2011.

[9] X. Li *et al.*, "An interactive platform to guide catheter ablation in human persistent atrial fibrillation using dominant frequency, organization and phase mapping," *Comput. Methods Progr. Biomed.*, vol. 141, pp. 83-92, Apr 2017.

[10] F.J. Vanheusden *et al.*, "Systematic differences of non-invasive dominant frequency estimation compared to invasive dominant frequency estimation in atrial fibrillation," *Comp. Biol. Med.*, vol. 104, pp. 299-309, Jan. 2019.

[11] J.L. Salinet *et al.*, "Analysis of QRS-T subtraction in unipolar atrial fibrillation electrograms," *Med. Biol. Eng. Comput.*, vol. 51, no. 12, pp. 1381-1391, Dec 2013.

[12] L.A Baccala *et al*,. "Directed transfer function: unified asymptotic theory and some of its implication," *IEEE Trans. Biomed. Eng.*, vol. 63, no. 12, pp. 2450-2460, Dec 2016.

Address for correspondence:

Frederique J Vanheusden
Department of Engineering, School of Science and Technology, Nottingham Trent University, New Hall Block 177, Clifton Campus, Clifton Lane, Clifton, Nottingham, NG11 8NS, UK
frederique.vanheusden@ntu.ac.uk